



Contents lists available at ScienceDirect

Bioorganic & Medicinal Chemistry Letters

journal homepage: www.elsevier.com/locate/bmcl

Biphenyl amide p38 kinase inhibitors 3: Improvement of cellular and in vivo activity

Richard Angell[†], Nicola M. Aston, Paul Bamborough, Jacky B. Buckton, Stuart Cockerill[†], Suzanne J. deBoeck, Chris D. Edwards, Duncan S. Holmes, Katherine L. Jones^{*}, Dramane I. Laine, Shila Patel[‡], Penny A. Smees, Kathryn J. Smith, Don O. Somers, Ann L. Walker

GlaxoSmithKline R&D, Medicines Research Centre, Gunnels Wood Road, Stevenage, Hertfordshire SG1 2NY, UK

ARTICLE INFO

Article history:

Received 9 May 2008

Revised 10 June 2008

Accepted 10 June 2008

Available online 18 June 2008

Keywords:

p38 Kinase

p38 Alpha

p38

CSBP

MAP kinase

Inhibitors

Biphenyl amide

BPA

Biphenyl amides

BPAs

Protein kinase X-ray structure

Binding mode

Structure-based drug design

Kinase selectivity

Structure–activity relationships

PG-PS model

CIA model

ABSTRACT

The biphenyl amides (BPAs) are a novel series of p38 α MAP kinase inhibitor. The optimisation of the series to give compounds that are potent in an in vivo disease model is discussed. SAR is presented and rationalised with reference to the crystallographic binding mode.

Published by Elsevier Ltd.

The biphenyl amides are a novel series of p38 MAP kinase inhibitor. Initial lead optimisation focused on optimisation of the amide substituent and of the 1,3,4-oxadiazole moiety.¹ Replacement of the oxadiazole by other heterocycles led, in most cases, to lower p38 α activity. However, the 4'-amide readily accommodated a wide range of different groups which provided improved enzyme and cellular potency and led to the discovery of **1**.

X-ray crystallography of **1** bound to the ATP-site of p38 α showed that the oxadiazole occupied a mainly lipophilic pocket, and that the nitrogen atoms on the oxadiazole formed hydrogen-

bonds to the kinase backbone at Asp168 and Phe169 in the DFG-motif.² The oxadiazole oxygen was positioned near the acid of the Glu71 sidechain. Modelling suggested that the isosteric replacement of the oxadiazole by an amide would maintain the hydrogen bond to Asp168 from the carbonyl oxygen, and in addition donate a hydrogen bond to Glu71 through the amide NH. The amide functionality also offered potential for increasing p38 α potency by optimisation of the interactions with the lipophilic pocket.

The synthesis of the compounds concentrated on two coupling reactions. The first connected amines to an acid core, to form benzamides **A**, while the second coupled acids to an amine core to give anilides **B** (Fig. 1).

Substituents were chosen with two goals in mind. The first was to probe the pocket filled by the oxadiazole in the X-ray complex of **1** using a range of similarly sized groups. The second was to try to access the “DFG-out” conformation of p38 α , first described in the

^{*} Corresponding author. Tel.: +44 1438 762914.

E-mail address: katherine.l.jones@gsk.com (K.L. Jones).

[†] Present address: Arrow Therapeutics, Britannia House, 7 Trinity Street, London SE1 1DA, UK.

[‡] Present address: University of Cambridge, Department of Biochemistry, Sanger Building, Old Addenbrookes Site, 80 Tennis Court Road, Cambridge CB2 1GA, UK.

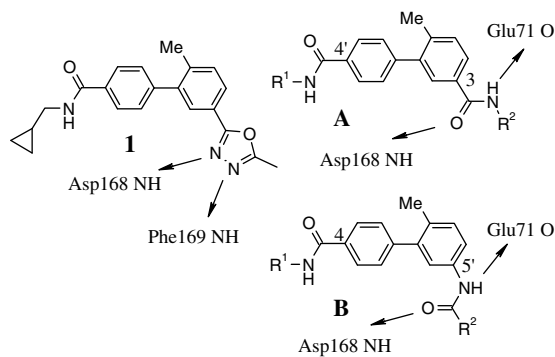


Figure 1. Benzamides (A) and anilides (B) showing ring numbering and p38 interactions.

literature for the complex of BIRB-796.³ Discussion here will be limited to biphenyl amides with the DFG-in binding mode: compounds with the DFG-out binding mode will be reported elsewhere.⁴

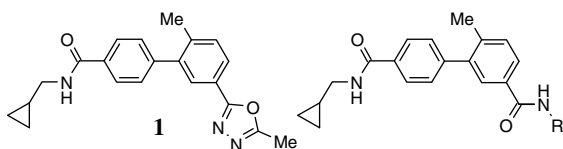
Appropriately substituted, both benzamides and anilides gave rise to potent inhibitors. Table 1 shows p38 α activity data for a range of benzamides, prepared as in Scheme 1.

The cyclopropyl amide **3** (K_i 12 nM) is one of the most potent inhibitors from the benzamide series. The X-ray structure of **3** complexed to p38 α was solved and is shown (Fig. 2) superimposed on that of **1** which has already been described.^{2,6} In the hinge region, the 4'-amides of **1** and **3** make the same hydrogen bond to Met109, and the substituents occupy the same region of the active site.

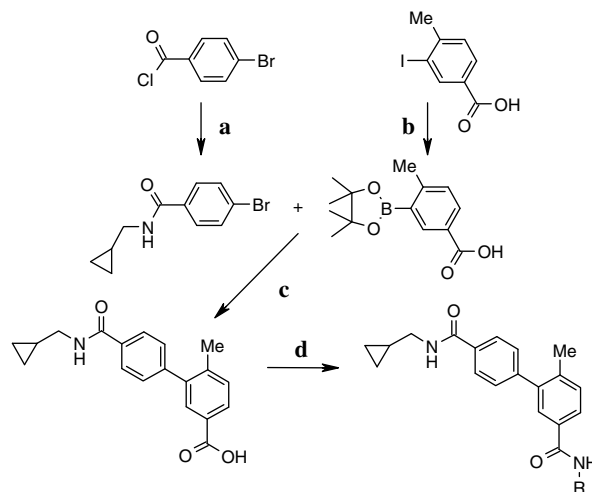
The two toluene rings overlay very closely. As expected, the oxygen of the 3-amide overlays closely with the N3 atom of the oxadiazole. Both accept hydrogen bonds from the backbone NH of Asp168. Compound **3** also donates an additional hydrogen bond from the 3-amide NH to the sidechain of Glu71.

The cyclopropyl group fits tightly in a lipophilic pocket, whose base is formed by the sidechains of Leu74 and Phe169, subtly rearranged from their positions in the complex with **1**. The sidechains of Glu71, Leu75 and Leu171 form the pocket walls. Small groups, such as the ethyl analogue (**2**), are less potent and would not fill this lipophilic pocket completely. Cyclopropyl has the greatest activity (**3**) which would indicate that it is a more optimal size. Longer aliphatic groups (e.g. **4**, **5**) show decreasing activity which

Table 1
Activities against p38 α of small benzamide analogues (nM)⁵



Compound	R	IC ₅₀	K _i
1	Not applicable	3000	480
2	Ethyl	610	100
3	Cyclopropyl	75	12
4	Propyl	970	150
5	Cyclopropylmethyl	550	90
6	Isobutyl	11000	1600
7	Cyclopentyl	2700	430
8	Cyclohexyl	8800	1400
9	Isopropyl	2500	400
10	Cyclobutyl	850	130
11	Phenyl	460	70
12	1,3-Thiazol-2-yl	86	14
13	1,3,4-Thiadiazol-2-yl	150	20



Scheme 1. Reagents: (a) cyclopropylmethylamine, NEt₃, THF, 74%; (b) bis(pinacolato)diboron, PdCl₂(dppf), KOAc, DMF 54%; (c) Pd(PPh₃)₄, 1 M Na₂CO₃ (aq), DME, 78%; (d) amide coupling, for example amine, HATU, DIPEA, DMF. (For **4** the order of amide formations was reversed.)

may be as a result of a clash with Leu74 or Phe169 in the pocket floor. Groups such as isobutyl, cyclopentyl and cyclohexyl (**6–8**) are weakly active. Although they would penetrate the pocket to a similar depth to **3**, they are wider and may clash with Glu71, Leu75 or Leu171 in the pocket walls. Groups of similar size to cyclopropyl such as isopropyl and cyclobutyl (**9**, **10**) are over 10-fold weaker than **3**, which further indicates the tight steric requirements.

Aromatic groups (**11–13**) also show size-dependent trends. The smaller 5-membered heteroaromatics (**12**, **13**) are more potent than phenyl (**11**).

Anilides (**B** (Fig. 1) were also synthesized (Scheme 2). X-ray complexes of several examples have been solved, and are very like the structure of **3** (data not shown). Both of the hydrogen-bonding interactions made between the amide linker and the protein are maintained, even though its direction is reversed. There is a slight shift in the position of the attached substituent resulting in different SAR for the two series of amides (Table 2).

As with the benzamides, activity against p38 α of compounds with the anilide alkyl substituents increases with size until the optimal size is reached, then rapidly decreases (**14–22**). Alkyl amides are weaker in the anilide series than in the benzamides. While the cyclopropyl substituted benzamide (**3**) is one of the most active compounds in that series, the cyclopropyl substituted anilide (**16**) is not particularly potent. Propyl (**17**) is the most active alkyl amide but is still threefold lower in activity than **3**. The anilides show a clear preference for aromatic substituents (**23–28**) which are more potent than their analogues in the benzamide series (compare **23** to **11**). Despite the good potency achieved in this series, the benzamides were preferred due to the potential toxicity risks associated with aniline formation during metabolism of the anilides.⁷

Variation at the 4' amide position (**29–37**), Table 3, was introduced into the benzamide series (Scheme 3). The 4'-amide substituent points towards solvent in a similar way to that of the 4'-amide of oxadiazole **1** and the SAR trends at this position in the amide series are very like those seen for the oxadiazoles.¹ A wide range of substitution on the 4'-amide is tolerated. Aryl and benzyl groups (**29–33**) show the greatest activity. Compounds from Table 3 were typically 50-fold more potent than the equivalent oxadiazoles.¹

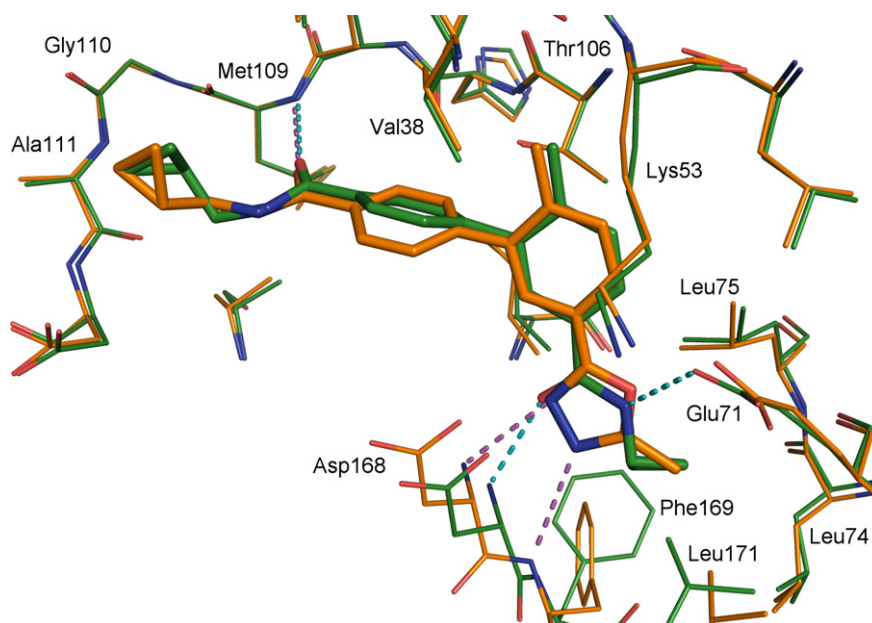
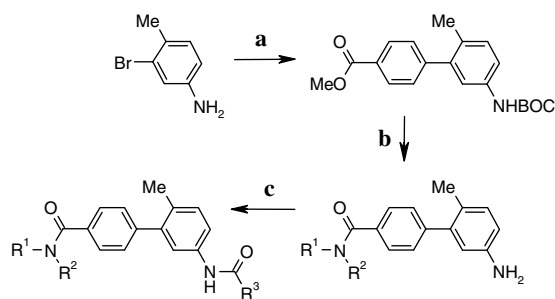


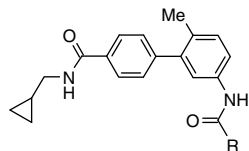
Figure 2. X-ray structure of **3** compared to **1** showing the 3-amide superimposed on the oxadiazole.



Scheme 2. Reagents: (a) i–di-*tert*-butyl dicarbonate, NEt_3 , DCM, 63%, ii–(4-methoxycarbonylphenyl)boronic acid, $\text{Pd}(\text{PPh}_3)_4$, CsCO_3 , DME, 97%; (b) i– NaOH , MeOH 49%, ii– HNR^1R^2 , HATU, DIPEA, THF, iii–TFA, DCM; (c) $\text{R}^3\text{CO}_2\text{H}$, CDI, THF/DMF.

Table 2

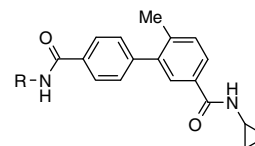
Activities against p38 α of small anilide analogues (nM)⁵



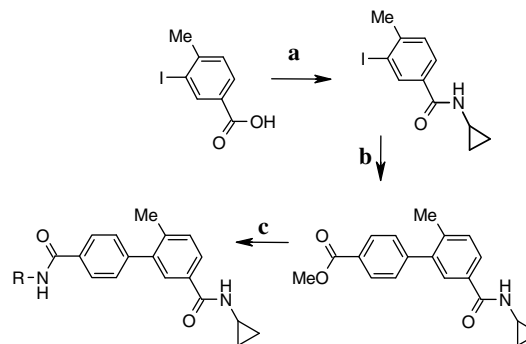
Compound	R	IC ₅₀	K _i
14	Methyl	4000	630
15	Ethyl	1100	170
16	Cyclopropyl	2300	350
17	Propyl	240	40
18	Cyclobutyl	1700	270
19	Cyclopropylmethyl	450	70
20	Isobutyl	2100	330
21	Cyclopentyl	7000	1100
22	Cyclohexyl	12000	1900
23	Phenyl	76	12
24	2-Furan	160	25
25	3-Furan	96	15
26	2-Thiophene	200	32
27	3-Thiophene	34	5
28	5-Isoxazole	40	6

Table 3

Activities against p38 α of small benzamide analogues (nM)⁵

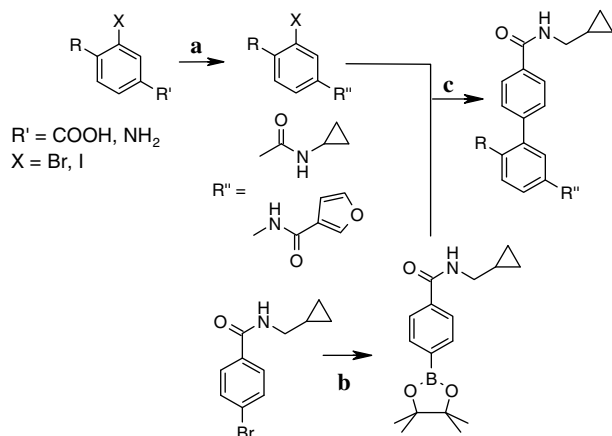


Compound	R	IC ₅₀	K _i
3	Cyclopropylmethyl	75	12
29	3-Cyanophenyl	33	5
30	4-Methoxyphenyl	42	7
31	3-Methoxybenzyl	23	4
32	3-[(Methylsulfonyl) amino]benzyl	10	2
33	4-(<i>N</i> -Me)piperazinyl benzyl	21	3
34	NH ₂	610	97
35	Propanol	270	43
36	Propylmorpholine	650	100
37	Dimethyl propylamine	230	370



Scheme 3. Reagents: (a) cyclopropylamine, HATU, HOBT, DIPEA, DMF; (b) (4-methoxycarbonylphenyl)boronic acid, $\text{Pd}(\text{PPh}_3)_4$, Cs_2CO_3 , DME; (c) i– NaOH , MeOH, H₂O, ii–various amide coupling conditions, for example amine, HATU, DIPEA, DMF.

The methyl on the toluene ring is one of the key requirements for p38 α activity in the series. As reported for the oxadiazole BPAs, modification in this region (**38–45**, Scheme 4) usually led to loss of

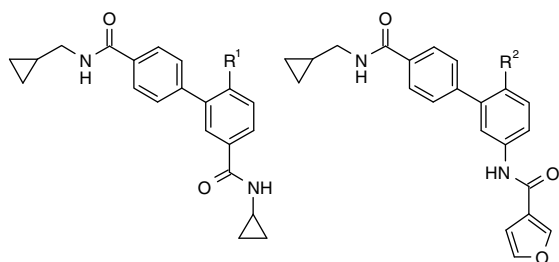


Scheme 4. Reagents: (a) HATU, HOBT, diisopropylethylamine, DMF, cyclopropylamine or 3-furoic acid; (b) bis(pinacolato)diboron, potassium acetate, PdCl₂(dppf), DMF; (c) Pd(PPh₃)₄, 2 M Na₂CO₃ (aq), DMF. (For **38** the boronic ester and halide were on opposite Suzuki coupling partners.)

activity as shown in Table 4.² Only chlorine was able to adequately replace methyl. When the methyl was replaced by smaller groups such as hydrogen or fluorine (**38**, **41**, **42**) the p38 α activity decreased by about 100-fold. Slightly larger groups, such as methoxy (**40**, **44**), caused a similar loss of potency. This data can be rationalised by studying the X-ray structure of **3**. The methyl appears to be the optimal size to fill the small lipophilic pocket formed by Ala51 and Thr106. Wedged against the beta sheet in the N-terminal lobe, this part of the site has little freedom to move in response to changes in the ligand. Compounds from Table 3 were typically 50-fold more potent than the equivalent oxadiazoles. This improvement is consistent with that seen for compound **3** over **1**, and can be rationalised in the same way.

Compounds from the bis-amide series had an improved profile over the oxadiazole series.¹ Compound **3** had a K_i of 12 nM,⁵ a significant improvement over the value of 480 nM for **1**. Compound **3** also inhibited the phosphorylation of ATF-2 by p38 α with a K_i of 10 nM.⁸ Selectivity was assessed by screening against a panel of 56 protein kinases. Only p38 α and p38 β (K_i = 24 nM) were significantly inhibited by **3**. The compound was at least 100-fold selective

Table 4
Activities against p38 α of methyl replacements (nM)⁵



Compound	R ¹	IC ₅₀	K _i
3	Me	75	12
38	H	>16,000	>2500
39	Cl	160	25
40	Methoxy	3300	520
41	Fluoro	2900	460
	R ²		
25	Me	96	15
42	H	5900	940
43	Cl	63	10
44	Methoxy	>16,000	>2500
45	Dimethylamine	>16,000	>2500

Table 5
Pharmacokinetic parameters of **3** measured in rat¹²

IV plasma clearance (ml/min/kg)	6
IV steady state volume of distribution (l/kg)	0.6
IV plasma terminal t _{1/2} (h)	1.3
Oral bioavailability	113%
Brain:plasma ratio	0.1–0.3

against AKT1, Aurora A, EGFR, EphB4, GSK-3 β , JNK3, Lck, ROCK1 and Syk. A similarly selective profile was observed for other members of the series. In addition, **3** was submitted to the KinomeScan assay panel, which measures binding against over 200 kinases or kinase domains fused to T7 bacteriophage.^{9a} Compound **3** only showed significant ability to displace an immobilised ATP-site ligand from p38 α and p38 β . This compares favourably to literature data for p38 inhibitors VX-745 and BIRB-796 which in a smaller panel were reported to bind to a number of off-target kinases.^{9b}

Compounds were profiled in a series of assays measuring the inhibition of a panel of p450 enzymes.¹⁰ Compound **3** was not a potent inhibitor of isoforms 1A2, 2C19, 2D6 or 3A4 (IC₅₀ > 10 μ M), but it did inhibit p450 2C9 with IC₅₀ of 4.4 μ M.

Along with other potent examples from the series, **3** was profiled in cellular assays. It was a very potent inhibitor of TNF- α release from peripheral blood mononuclear cells with IC₅₀ of 250 nM, a considerable improvement over **1** (2.5 μ M).¹¹ In addition, **3** reduced the level of TNF α in response to LPS-stimulation of whole blood with IC₅₀ = 1 μ M.¹¹

Compound **3** had good pharmacokinetic properties in the rat (Table 5).¹² Oral bioavailability was excellent, with low clearance and a moderate volume of distribution. The compound also showed a low brain:plasma ratio, which would reduce any risk of unwanted activity in the CNS.

Interestingly, the cyclopropylamide amide replacement (**3**) for the methyl-oxadiazole (**1**) seemed to boost further the oral bioavailability of **3**, despite the additional hydrogen bond donor (**1** showed oral bioavailability of 50% and similar clearance to **3**).¹ However, the substitution did not affect the brain penetration in the rat, which was low for both compounds (brain:plasma ratio for **1** was 0.3). A potential explanation for these findings is that the complete oral bioavailability of **3** may have been driven by a slightly improved solubility over **1**, or may have been determined by a different impact of active component of intestinal absorption, rather than by simple passive transcellular absorption.

In addition, compound **3** showed excellent activity in a rat PG-PS (peptidoglycan-polysaccharide) reactivation model, with ED₅₀ = 0.02 mg/kg.² This compared favourably with **1** (ED₅₀ = 15 mg/kg) and prednisolone (ED₅₀ = 1 mg/kg). It was also tested in a mouse collagen induced arthritis (CIA) model of rheumatoid arthritis,¹³ in which it totally prevented the progression of arthritis at 15 mg/kg/day. At the higher dose of 30 mg/kg/day, it had a beneficial effect on arthritis and reduced clinical score compared to the level at the start of the dosing period. In this model **3** compared favourably with Enbrel, soluble recombinant TNF receptor, dosed at 300 μ g ip on alternate days, which reduced inflammation but did not completely prevent disease progression.

In conclusion, replacement of the oxadiazole ring of the early biphenyl amide p38 α inhibitors led to a series of compounds with greatly improved properties, including excellent cellular potency, pharmacokinetic properties and oral activity. Future publications will describe the continuing optimisation of the series to yield candidate quality molecules.

Acknowledgements

The authors thank Rick Williamson and Giovanni Vitulli for suggestions and for contributing experimental details, Tony Cooper,

Rachel Hosking and Steve Flack for synthesis of compounds, Vipul Patel for helpful discussions, and all other members of the p38 team for their many contributions.

References and notes

- Angell, R. M.; Angell, T. D.; Bamborough, P.; Brown, D.; Brown, M.; Buckton, J. B.; Cockerill, S. G.; Edwards, C. D.; Jones, K. L.; Longstaff, T.; Smees, P. A.; Smith, K. J.; Somers, D. O.; Walker, A. L.; Willson, M. *Bioorg. Med. Chem. Lett.* **2008**, *18*, 324.
- Angell, R. M.; Bamborough, P.; Cleasby, A.; Cockerill, S.; Jones, K. L.; Mooney, C. J.; Somers, D. O.; Walker, A. L. *Bioorg. Med. Chem. Lett.* **2008**, *18*, 318.
- Pargellis, C.; Tong, L.; Churchill, L.; Cirillo, P.; Gilmore, T.; Graham, A.; Grob, P.; Hickey, E.; Moss, N.; Pav, S.; Regan, J. *Nat. Struct. Biol.* **2002**, *9*, 268.
- Angell, R.; Aston, N.M.; Bamborough, P.; Buckton, J.B.; Cockerill, S., de Boeck, S.J.; Edwards, C.D.; Holmes, D.S.; Jones, K.L.; Laine, D.I.; Patel, S.; Smees, P.A.; Smith, K.J.; Somers, D.O.; Walker, A.L.; *Bioorg. Med. Chem. Lett.*, accepted for publication.
- Enzyme IC_{50} and K_i determination, using an assay measuring displacement of a fluorescent ATP-competitive inhibitor was carried out as described in reference 1.
- An *apo* crystal of unphosphorylated human p38 α (expressed, purified and crystallized as previously described) was soaked with 0.25 mM **3** for 1 day and cryoprotected as for compounds **3** and **4** of the previous publication.² X-ray diffraction data were collected from the crystal at 100 K (using an Oxford Cryostream) on a Rigaku-MSR RuH2R rotating anode X-ray generator with a RAXIS IV++ image-plate detector. The data were processed with the HKL package (Otwinowski, Z.; Minor, W. *Methods Enzymol.* **1997**, *276*:Macromol. Cryst. A, 307–326) and CCP4 program suite (Bailey, S. *Acta Crystallogr., Sect. D*, **1994**, *50*, 760–763). The structure was solved using the native p38 coordinates (PDB entry 1WFC) as the initial model in refinement by REFMAC (Murshudov, G.; Vagin, A.; Dodson, E. *Acta Crystallogr., Sect. D*, **1997**, *D53*, 240–255). The final R-factor achieved for the complex was 17.4%. Coordinates have been deposited in the PDB as entry 3D7Z.
- (a) Harrison, J. H., Jr.; Hollow, D. J. *J. Pharmacol. Exp. Ther.* **1986**, *238*, 1045; (b) Osazaki, Y.; Yamashita, K.; Ishii, H.; Sudi, M.; Tsuchitani, M. *J. Appl. Toxicol.* **2003**, *23*, 315.
- Recombinant His-tagged human p38 α was activated using 3 μ M unactivated p38 α incubated in 200 mM Hepes pH 7.4, 625 mM NaCl; 1 mM DTT with 27 nM active MKK6 (Upstate). Activity of the activated p38 α was assessed using a time-resolved fluorescence energy transfer (TR-FRET) assay. Biotinylated GST-ATF2 (residues 19–96, 400 nM final), ATP (125 mM final) and $MgCl_2$ (5 mM final) in assay buffer (40 mM HEPES pH 7.4, 1 mM DTT) were added to wells containing 1 μ l of various concentrations of compound or DMSO vehicle (3% final) in NUNC 384-well black plate. The reaction was initiated by addition of p38 α (100 pM final) to give a total volume of 30 μ l. After 120 min incubation (rt), 15 μ l of 100 mM EDTA pH 7.4 was added followed by detection reagent (15 μ l) in buffer (100 mM HEPES pH 7.4, 150 mM NaCl, 0.1% w/v BSA, 1 mM DTT) containing anti-phosphothreonine-ATF2-71 polyclonal antibody (Cell Signalling Technology, Beverly, Massachusetts, MA) labelled with W-1024 Eu chelate (Wallac OY, Turku, Finland), and APC-labelled streptavidin (Prozyme, San Leandro, CA). After 60 min further incubation (rt) the ATF-2 phosphorylation was measured using a Packard Discovery plate reader (Perkin-Elmer, Pangbourne, UK) as a ratio of specific 665 nm energy transfer signal to reference Eu 620 nm signal. To calculate K_i from determined IC_{50} the Cheng-Prusoff equation was used (Ref. 1), $K_i = IC_{50}/(1 + ([S]/K_m))$.
- Assays were carried out by Ambit Biosciences, San Diego. The ability of compounds to compete with the binding of the human kinase (expressed as fusion to T7 bacteriophage) to immobilized ATP-site probe ligands was determined as previously described, see: (a) Fabian, M. A.; Biggs, W. H., III; Treiber, D. K.; Atteridge, C. E.; Azimioara, M. D.; Benedetti, M. G.; Carter, T. A.; Ciceri, P.; Edeen, P. T.; Floyd, M.; Ford, J. M.; Galvin, M.; Gerlach, J. L.; Grotzfeld, R. M.; Herrgard, S.; Insko, D. E.; Insko, M. A.; Lai, A. G.; Lélias, J.-M.; Mehta, S. A.; Milanov, Z. V.; Velasco, A. M.; Wodicka, L. M.; Patel, H. K.; Zarrinkar, P. P.; Lockhart, D. J. *Nat. Biotechnol.* **2005**, *23*, 329. Compounds were screened at 10 μ M and considered active if <10% of binding to immobilised probes remained compared to DMSO control.; (b) Goldstein, David M.; Gabriel, Tobias *Curr. Topics Med. Chem.* **2005**, *5*, 1017.
- The inhibition of recombinant CYP450 mediated O-dealkylase metabolism of pro-fluorescent probe substrates were assessed in a fluorimetric assay with the following recombinant human cytochrome P450s co-expressed in *Escherichia coli* with human NADPH reductase (Bactosomes, CYPEX, UK); CYP2C9 with the substrate 7-methoxy-4-trifluoromethylcoumarin-3-acetic acid (FCA); CYP1A2 with the substrate ethoxyresorufin (ER); CYP2D6 with the substrate 4-methylaminomethyl-7-methoxycoumarin (MMMC); CYP2C19 with the substrate 3-butyryl-7-methoxycoumarin (BMC); and CYP3A4 with the substrates 7-benzoxoquinolone (7BQ) and diethoxyfluorescein (DEF). Compounds were prepared as 5 mM MeOH stock solutions with final incubations containing <2% MeOH. The concentration range for the IC_{50} determination assay was 0.1–100 μ M (spread over 9 points) and included a 0.2 mM NADPH regeneration system.
- (a) Inhibition of LPS-stimulated TNF α release was measured in isolated peripheral blood mononuclear cells as described in Ref. 1. (b) Inhibition of TNF α release in response to LPS-stimulation was carried out in whole blood. Heparinised blood drawn from normal volunteers was dispensed (100 μ l) into microtitre plate wells containing 0.5 or 1.0 μ l of an appropriately diluted compound solution. After 1 h incubation at 37 °C, 5% CO₂, 25 μ l LPS solution in RPMI 1640 (containing 1% l-glutamine and 1% penicillin/streptomycin) was added (50 ng/ml final). The samples were incubated at 37 °C, 5% CO₂ for 20 h, 100–150 μ l physiological saline (0.138% NaCl) was added and diluted plasma was collected using a Platamate or Biomek FX liquid handling robot after centrifugation at 1300g for 10 min. Plasma TNF α content was determined by enzyme linked immunosorbent assay (ELISA) or using a multiplex bead technology (Luminex).
- Pharmacokinetic parameters in male Lewis rats were determined following intravenous (iv) and oral (po) administration at 0.5 mg/kg and 1.5 mg/kg, respectively. Compound was administered as a solution in 10% DMSO: 45% SBE Cyclodextrin, 45% MSA (IV) or 5% DMSO, 40% vitE, 40% PEG200, 15% Mannitol (po). Blood was collected over a 24-h time period. Plasma was prepared following centrifugation and compound extracted from 50 μ l plasma using protein precipitation with acetonitrile. Samples were then evaporated under nitrogen and re-suspended in 100 μ l of 10:90 acetonitrile/water. Analysis was performed using LC-MSMS on the API365 with a 5 min fast gradient comprising 0.1% formic acid in water and 0.1% formic acid in acetonitrile (mobile phases), 20 μ l injection volume, flow rate 4 ml/min and ODS3 Prodigy column (5 cm \times 2.1 mm, 5 μ m). Pharmacokinetic data was generated using a non-compartmental approach. The brain penetration was assessed in the Lewis rat, collecting brains and terminal blood samples five minutes after an intravenous administration at 1 mg/kg, using the same formulation as in the intravenous PK study. Brains were homogenised in a water:methanol 1:1 solution and the homogenates analysed with a protein precipitation method similar to the one detailed for plasma analysis.
- CIA is a widely used animal model of arthritis in which the anti-inflammatory and anti-rheumatic efficacy of drugs and novel compounds predicted to have activity in RA are evaluated. This model is one of the more widely used animal models of RA and shares many similarities with the human disease, for example synovial hyperplasia, infiltration of inflammatory cells, erosion of cartilage and bone and involvement of both B and T lymphocytes. It has extensively been reported in the literature that CIA can be inhibited by anti-cytokine reagents (IL-1b, IL-6 and to a lesser extent TNF α). CIA was induced by sensitising DBA/1 mice against bovine type II collagen + Freund's Complete adjuvant injected intradermally at the base of the tail followed 3 weeks later by an intraperitoneal booster injection of bovine type II collagen. The activity of compound **3** in this model was assessed by orally dosing mice twice daily for 14 days with 15 or 30 mg/kg starting when the mice were showing early signs of inflammation in the paws. Enbrel (soluble TNF α receptor) was tested in the same study as a comparator. Clinical scores were monitored throughout the dosing period as a measure of anti-inflammatory effect and at the end of the study, ankle joints were processed histologically to assess effects on structural damage.